Metal Artifact Reduction for Orthopedic Implants (O-MAR)

Summary

Since the inception of CT, numerous methods have been proposed to suppress metal artifacts with varying degrees of success.[1-4] O-MAR (Metal Artifact Reduction for Orthopedic Implants) is a commercial product available from Philips Healthcare which implements a robust and efficient algorithm to mitigate artifacts caused by metal objects in CT images. This work provides an overview of this novel algorithm, its usability and will include a quantitative analysis of its application for images of a phantom. Several examples of O-MAR with different anatomies and implant types will be covered. There are instances where O-MAR may induce artifacts and is therefore contraindicated. These cases are described in this document.

Background

The presence of high atomic number (high-Z) materials (e.g. prosthetics, dental fillings) in CT images may cause severe artifacts. These artifacts exhibit themselves as streaks, dark areas in the image and overall obscuring of data. The source of these artifacts are beam hardening effects, photon starvation and the application of filtered backprojection in the presence of sharp gradients in the sinogram data. Beam hardening is due to the polychromatic composition of the CT x-ray beam. As the beam passes through an object, more low energy photons are absorbed as compared to high energy photons. The energy mix of the beam is now modified and it contains proportionately more high energy (i.e. more penetrating) photons, hence, the term beam hardening. As a result of beam hardening, x-ray absorption is non-linear with distance. This effect can be rectified by applying a polynomial correction to the raw data. This correction is adequate for a single material object like water or an object containing materials of similar x-ray attenuation like tissue. However, the combination of metal and tissue will cause this correction to be inaccurate and produce artifacts.

Since metal has a high attenuation, x-rays passing through metal will have low photon flux at the detectors. Sometime this flux is so low, the detectors are 'starved' for photons and do not produce a signal thereby causing incorrect calculations during the reconstruction process. Even when sufficient photons are received by the detectors, due to the high attenuation of metal, the quantum noise is much higher as compared to projections that do not pass through the metal. These noisy projections will result in streaks in the CT image.

PHILIPS

sense and simplicity

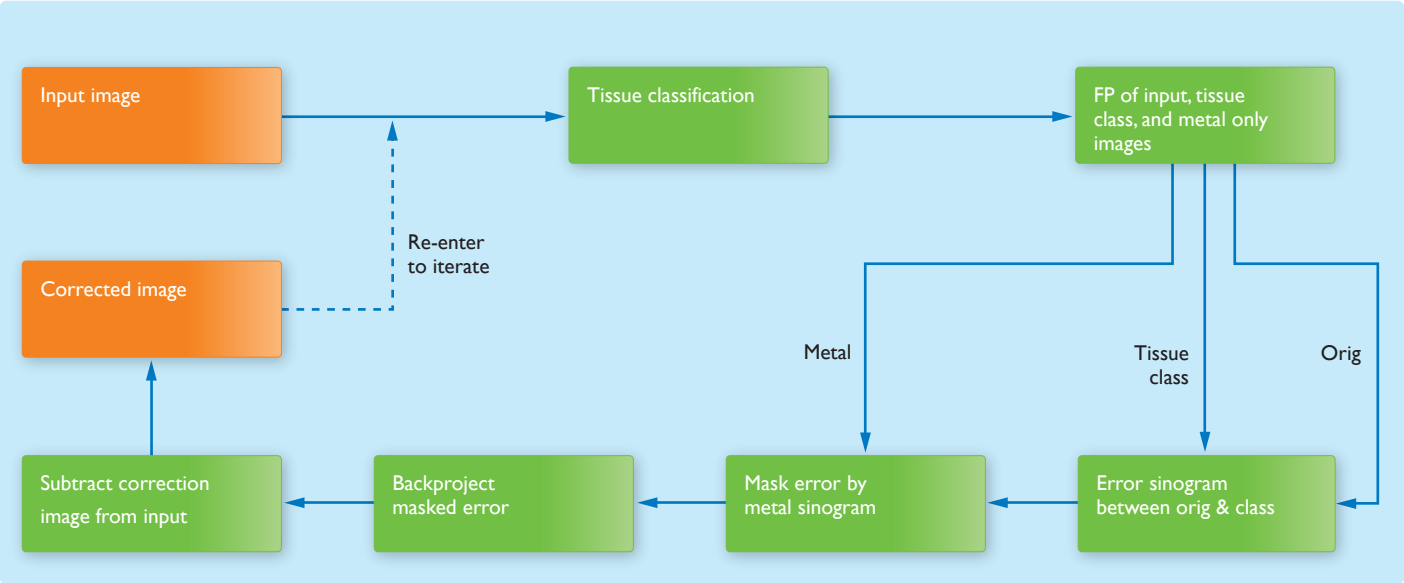

Figure 1

Algorithm description

The crux of the O-MAR implementation is an iterative loop where the output correction image is subtracted from the original input image. The resultant image can then become the new input image and the process can be repeated. A system diagram of this technique is shown in Fig. 1. The first step is to threshold the input image to create a metal only image. The metal only image consists of all pixels set to zero except for those pixels categorized as metal. This image will be used to identify the projections within the sinogram data that have contributions from metal. If no large clusters of metal pixels are present in the image, no further processing is performed. Therefore, O-MAR has no impact on non-metal images. Furthermore, O-MAR will not be applied to stents or similar small metal objects.

A tissue classified image is created by segmenting the input image into tissue and non-tissue pixels. All pixels within a Hounsefield unit (HU) range near 0 are classified as tissue. All tissue pixels are set to a single value and all other pixels left unmodified. The HU for tissue is the average of all tissue pixels. See Fig. 2. The metal only, tissue classified and input images are all forward projected (FP) to generate the corresponding sinogram data.

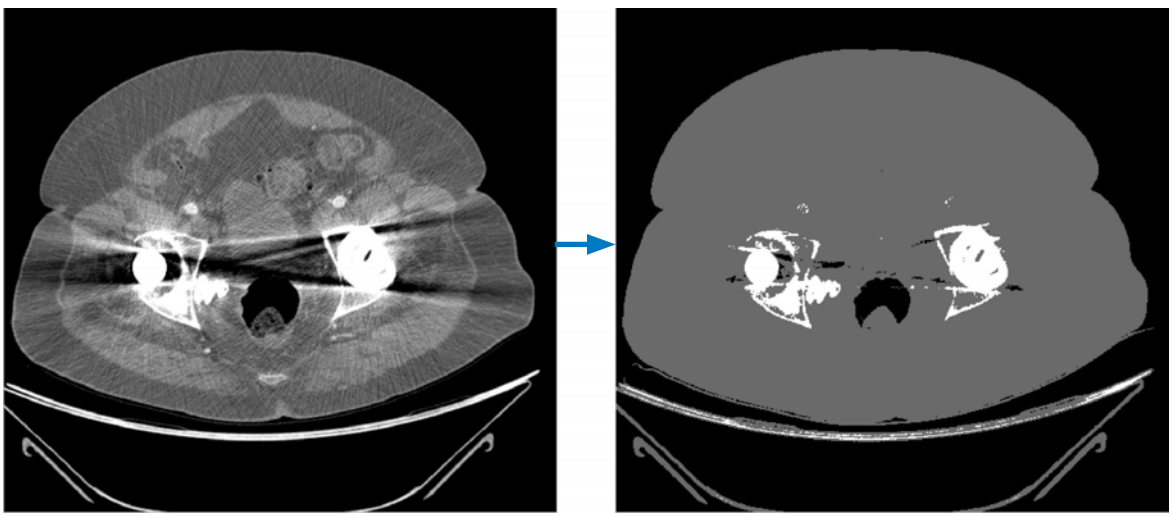

Original Tissue classified

Figure 2

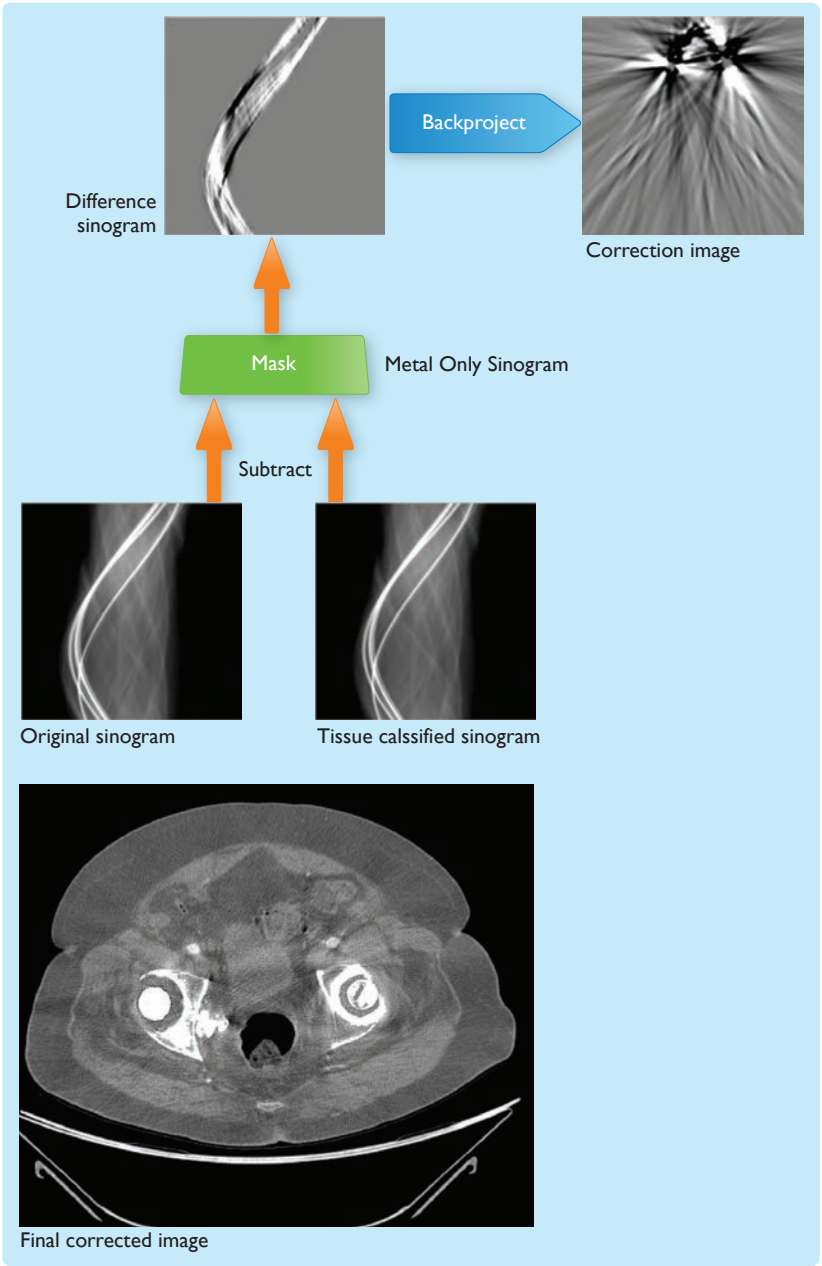

Figure 3

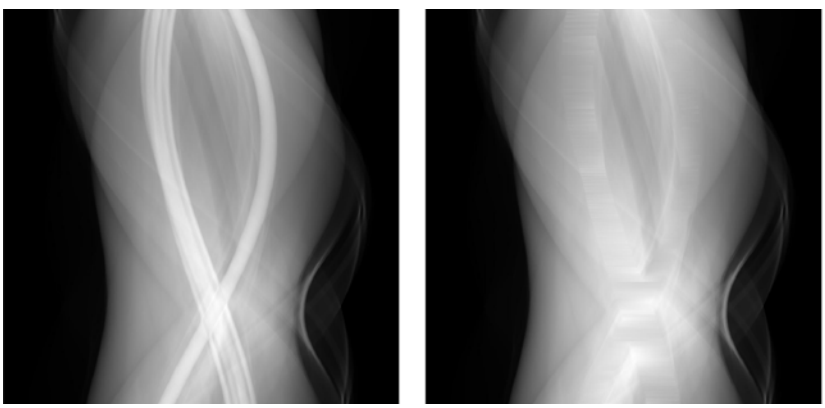

Original sinogram Metal replaced

Figure 4

The tissue classified sinogram is subtracted from the original image sinogram which produces an error sinogram. The metal sinogram data is now utilized as mask to remove all of the non-metal data points from the error sinogram. This error sinogram data is backprojected to generate the correction image. See Fig. 3.

An innovative aspect of this algorithm is in the first iteration. The tissue classified image is not produced from the original uncorrected image. Rather the metal data points in the sinogram are identified and removed. These points are replaced with interpolated values which will simulate tissue in place of the metal. See Fig. 4. This sinogram is backprojected and the resultant image is used to segment tissue and create the tissue classified image. For subsequent iterations, this step is not performed.

This complex process is embedded within the reconstruction system on the CT scanner. From a user's perspective, the O-MAR feature is invoked by a simple check box on the CT image acquisition console. When O-MAR is selected by the user, the system will execute the O-MAR algorithm to process the raw data. A clinician should compare the O-MAR images with the conventional data set. Therefore, the system will always reconstruct and store the uncorrected images in addition to the O-MAR processed images. Since there is a possibility though rare that O-MAR may induce an artifact, it is imperative that uncorrected images be referenced before making a definitive diagnosis. The system provides the uncorrected data volume automatically and no user action is required. When these data sets are displayed on CT console and other Philips workstations, the O-MAR images will have the text O-MAR displayed in the lower left hand corner. Additionally, this text will be prepended to the following public DICOM tags:

- Series Description [0008, 103E]
- Image Comments [0020,4000]

O-MAR images will be distinguishable on any PACS or Radiation Therapy Planning (RTP) system that displays these tags.

Phantom Studies

To provide a quantitative analysis of O-MAR, several experiments were performed with metal in a CT phantom. A 15mm steel bolt was inserted into the standard Brilliance Big Bore phantom. Several scans were performed using 90,120,140 kVp's and varying levels of mAs. Identical scans were performed on the phantom with the bolt removed. Circular ROI's (regions of interest) were drawn at identical locations on all images and the average HU and standard deviation (SD) were computed.

90kV	120kV	140kV	CTDI
N/A	50mAs	35mAs	3.0mGy
228mAs	100mAs	68mAs	5.9mGy
674mAs	300mAs	204mAs	17.8mGy
1135mAs	500mAs	340mAs	29.6mGy
2271mAs	1000mAs	678mAs	59.2mGy

Table 1

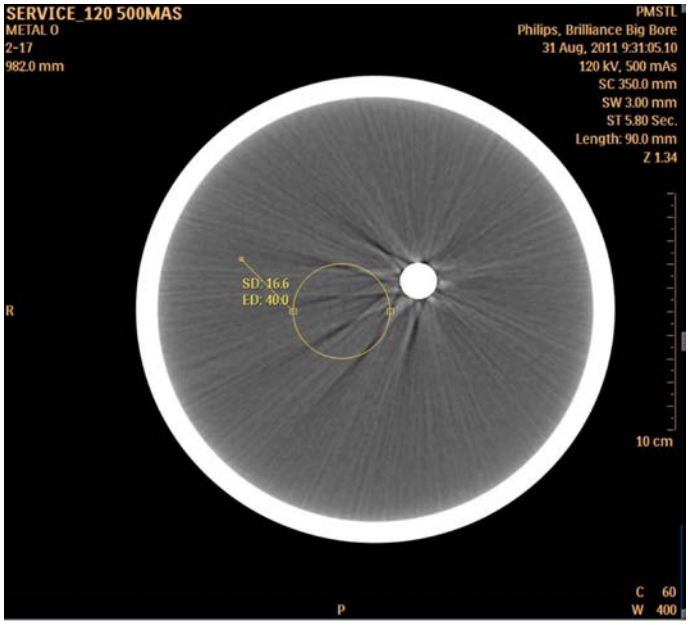

Figure 5

The mAs values were selected for the 120kVp scans. The mAs for the other kVp's were adjusted to be CTDI dose equivalent to the 120kVp scans. This approach allows the non-metal or background noise to be equivalent for all kVp's. The mAs used are listed in Table 1. The 90kVp/50mAs was extremely noisy and was excluded in order to not skew the plot of the results. An ROI with a 4cm diameter was drawn at the center of the slices. This position was chosen because of its proximity to the steel bolt and it includes a significant sampling of the metal streak artifacts. The center of the image is also an area with the lowest statistical noise. See Fig. 5. The SD of the HU within this ROI is used as an indicator of the severity of the metal artifacts. Both the uncorrected and O-MAR images were analyzed.

In figure 6, is an example of identical slices reconstructed with and without O-MAR. The 4cm ROI is drawn at the exact same location in both images. In this case, the reduction of SD from the non-O-MAR to O-MAR image was 12.4 to 6.3 HU.

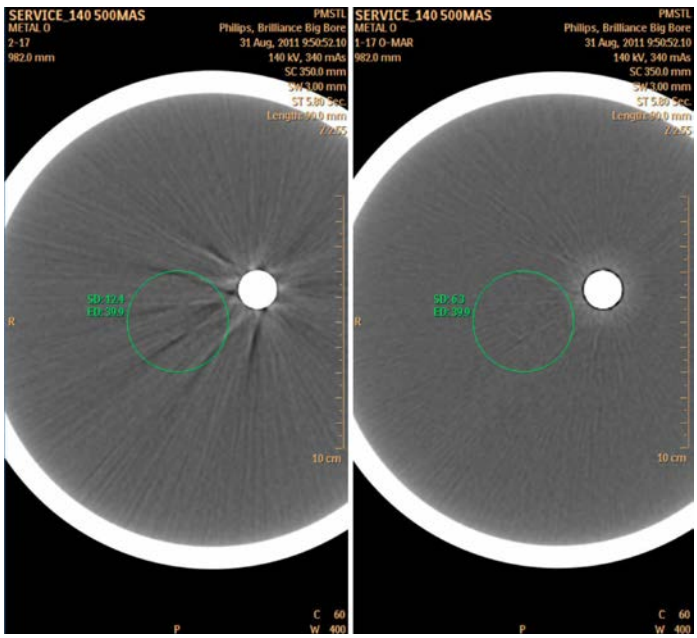

Figure 6 120kVp,500mAs uncorrected and O-MAR.

The SD values for uncorrected metal and O-MAR images are shown in Graph 1. A plot of the noise in a plain water phantom (i.e. no metal) is also included. Note, these SD values for the non-metal phantom are independent of kVp, since the mAs was adjusted to be dose (i.e. CTDI) equivalent.

Though using a plain water phantom with a cylindrical bolt may seem to be a trivial example, several insights into the metal artifact mechanism can be derived from these experiments.

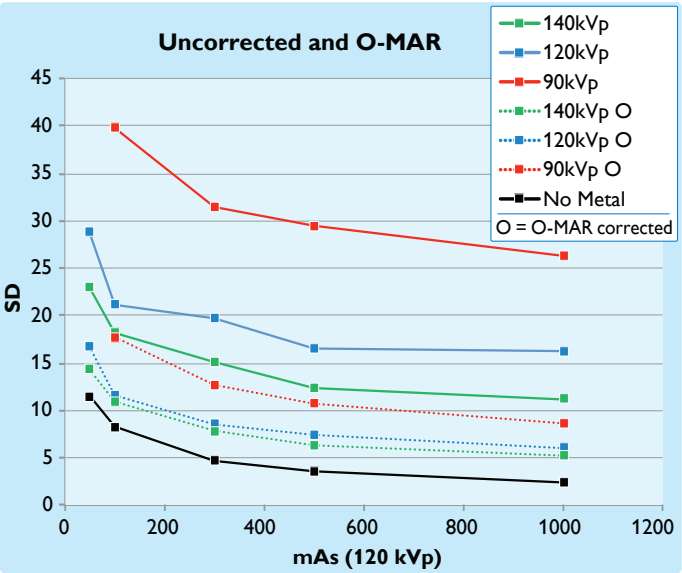

Graph 1

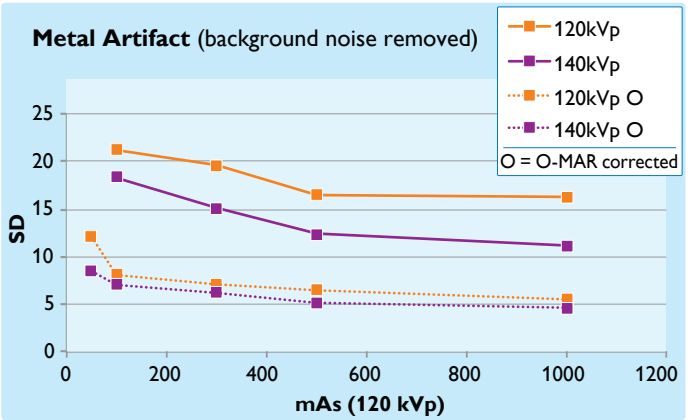

Graph 2

Instead of directly comparing the non-O-MAR and O-MAR images strictly using the measured SD, it would be more accurate to remove the bias of the background noise in these cases. A more proper evaluation involves the principle that the noise due to an artifact is governed by the following equation:[5]

$$Artifact = \sqrt{SD_a^{\,2} - SD_b^{\,2}}$$

Where SD_a is the measured noise with the artifact present and SD_b is the background noise which for purposes of this analysis is the SD (noise) of the phantom without the metal insert. After re-computing the data collected above to remove the bias of the background noise, the non-O-MAR and O-MAR results are plotted above. The 90kVp data was suppressed because it is consistently much more metal artifact prone and tends to skew the graphs (see Graphs 1 and 2).

Discussion

- The O-MAR correction can yield salient improvements in image quality even in the presence of severe background noise.
- Using a higher kVp will facilitate the ability of the O-MAR algorithm to reduce metal induced artifacts. Whenever possible, 140kVp should be utilized when orthopedic metal is present.
- If the mAs is held constant increasing the kVp from 120 to 140 will significantly improve the image quality of the O-MAR images. Raising the kVp to 140kVp not only decreases the impact of beam hardening, it also lessens statistical noise which benefits the O-MAR algorithm

Patient Images

Though O-MAR does not totally eliminate metal artifacts as shown in the section above, it is capable of reducing its effect on CT images to significantly enhance the diagnostic quality of the images. In this section, several different combinations of anatomy and orthopedic metal will be analyzed to demonstrate the clinical efficacy of O-MAR using real patient data.

With the increasing elderly population, it is now common to CT scan patients with an orthopedic hip prosthesis. This large metal object can cause severe metal artifacts in the CT images. In Fig. 7, is an example and the diagnostic improvement with O-MAR is self evident. Both the streak and darkening artifacts have been mitigated.

A more challenging case is a patient that has a dual hip prosthesis. This will result in a large area of dark pixels in the center of the anatomy. This practically precludes any useful diagnosis from those slices impacted by the metal. In Fig. 8, is an example of the capabilities of O-MAR in this extremely challenging situation. On these images several ROI's were drawn and the average HU and SD are displayed. The O-MAR image HU are closer to typical values for soft tissue thus demonstrating that the HU integrity is maintained with O-MAR. Note, the ROI on the patient's right within muscle tissue. A typical HU for this area is ~55. The O-MAR HU of 69.3 is more plausible than the 149HU seen on the uncorrected image.

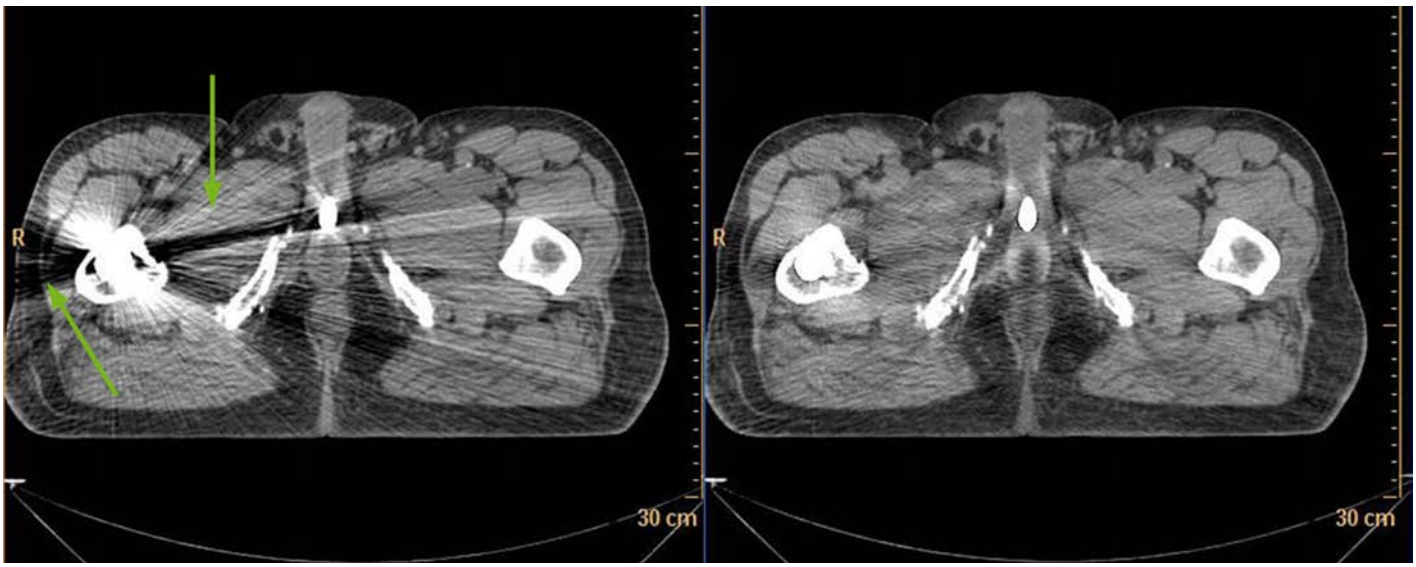

Uncorrected O-MAR

Figure 7

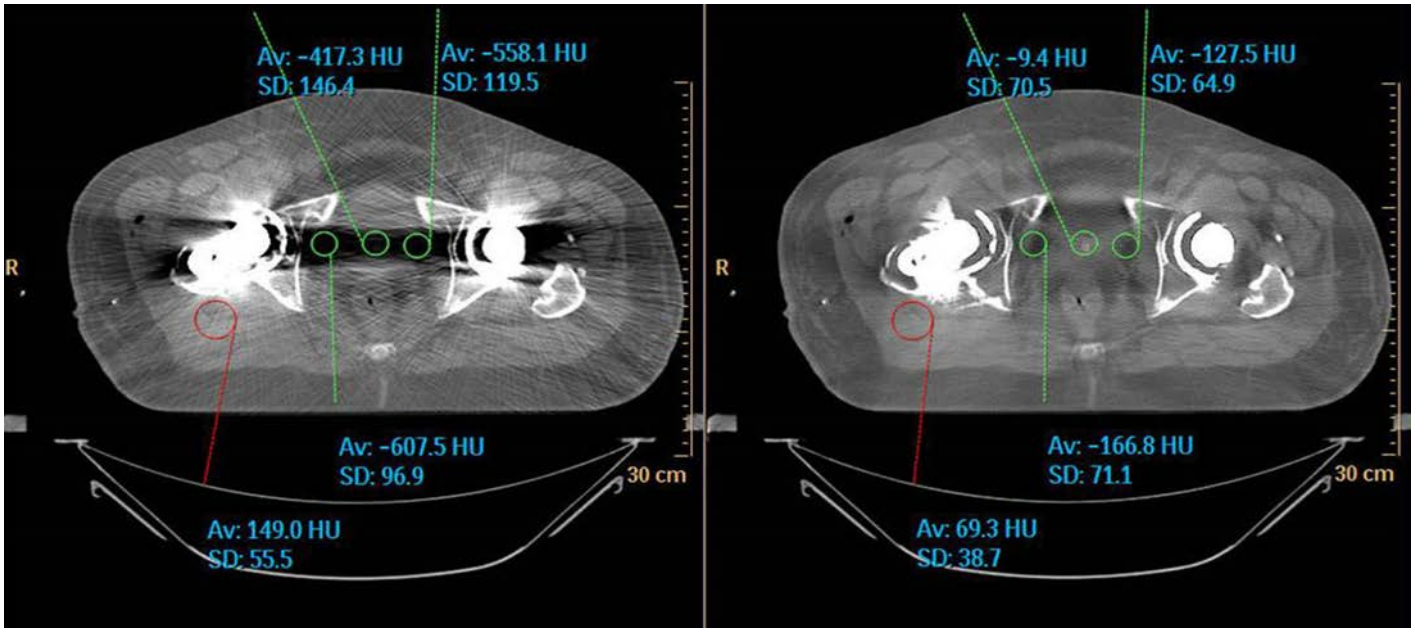

Uncorrected O-MAR

Figure 8

Uncorrected	O-MAR
-607.5	-166.8
-417.3	-9.4
-558.1	-127.5

Average HU of ROI's in center

Imaging of extremities can also be hampered by metal. Fig. 9 is an example of an orthopedic implant in the left leg of a patient. With O-MAR the muscle tissue near the implant is no longer obscured.

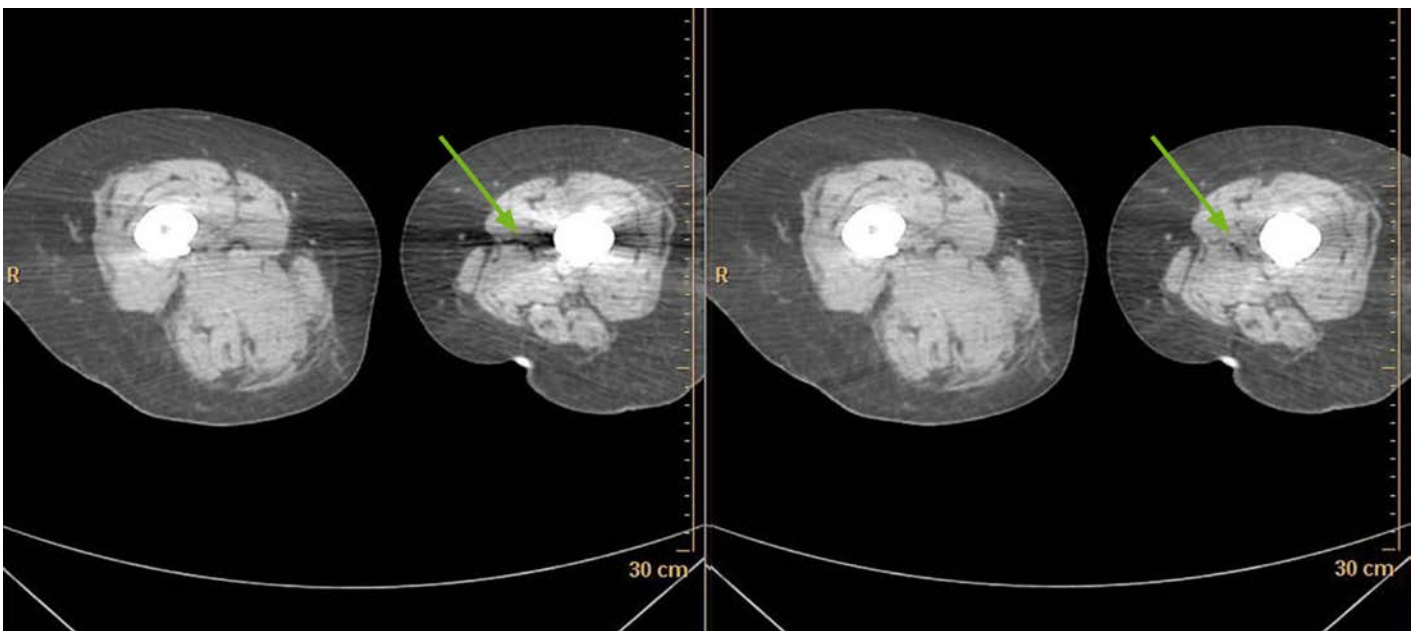

Uncorrected O-MAR

Figure 9

Metal artifacts not only impact 2-D slices. Sometimes 3-D volume rendered images will also display anomalies caused by metal. For example, Fig. 10 has an orthopedic humerus. In the uncorrected image the streaks from the metal object obscure the implant's attachment to the shoulder. On the O-MAR image, the metal bone interface is clearly visible.

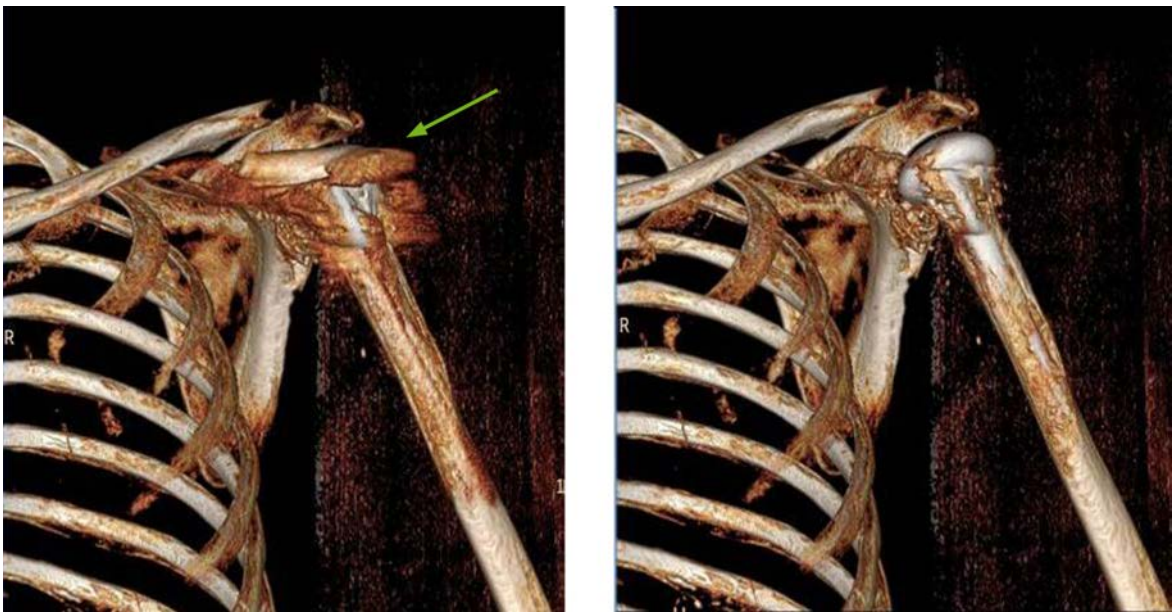

Uncorrected O-MAR

Figure 10 Metal humerus.

The main purpose of O-MAR is to address artifacts arising from orthopedic metal. However, it is also effective for non-orthopedic metal e.g. dental filings. Fig. 11 is an example of O-MAR being applied to a patient with a dental crown. Not only is soft tissue anatomy more discernable, the skin boundary is more detectable. This is important for Radiation Therapy Planning (RTP) where automatic algorithms are often employed to identify the skin contour. Without O-MAR these automatic methods would fail, requiring the user to manually correct the external contour.

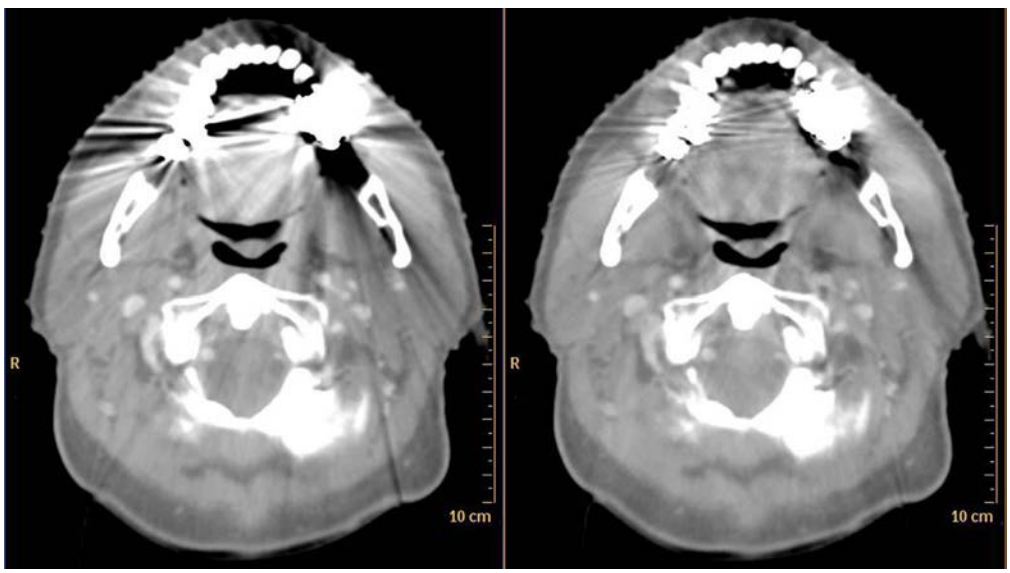

Uncorrected O-MAR

Figure 11

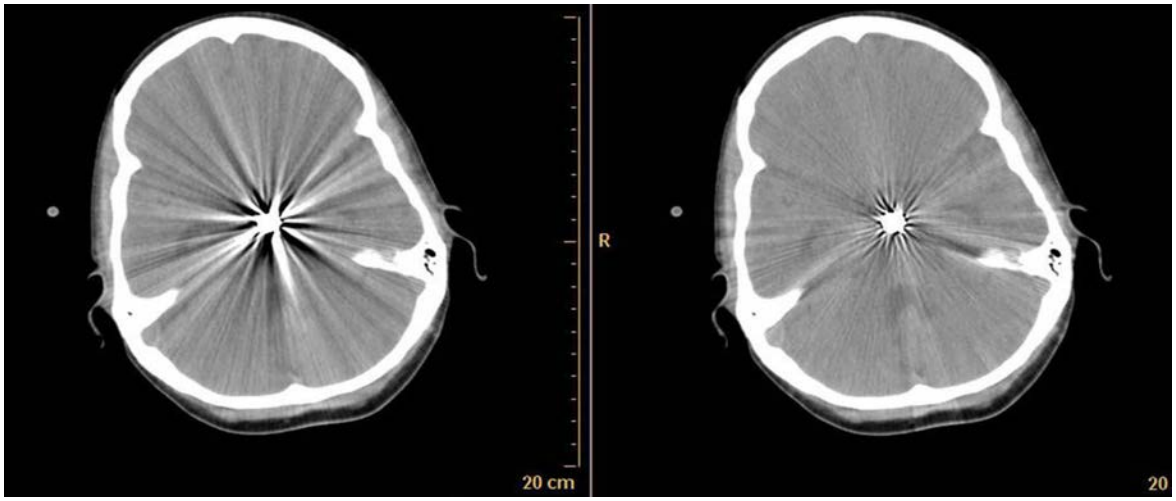

Uncorrected O-MAR

Figure 12

Another example of non-orthopedic metal is metal discs in brain scans, which can cause severe artifacts. For these cases, O-MAR is also very effective as can be seen in Fig. 12. In the O-MAR image, the fourth ventricle and the horns of the lateral ventricles are quite evident while on the uncorrected image these regions are nearly obscured by the metal artifact streaks.

Radiation Oncology

When CT is used for RTP, it is vital that the tumor and organs at risk (OAR) be accurately identified and delineated. Orthopedic implants can become a more critical impediment in this venue. Below (see Fig. 13) is an example of a bladder that was contoured by the same physician on both the O-MAR and uncorrected images. The O-MAR generated contour is in red and the contour from the uncorrected image is in green. On the uncorrected images the bladder was mostly obscured by the dark shadow caused by metal, therefore the physician overestimated the size of the bladder. On the O-MAR images, the bladder boundary was visible. There was no inter-observer variability and the contoured volumes differed by 32%. This is one sample of a more comprehensive and controlled study that is currently in progress at Henry Ford Health Systems. To fully cover all of the implications of O-MAR in radiation oncology, further analysis is required on dosimetric impact of contour differences and the potential improved accuracy of heterogeneity correction. This is being planned for a future paper.

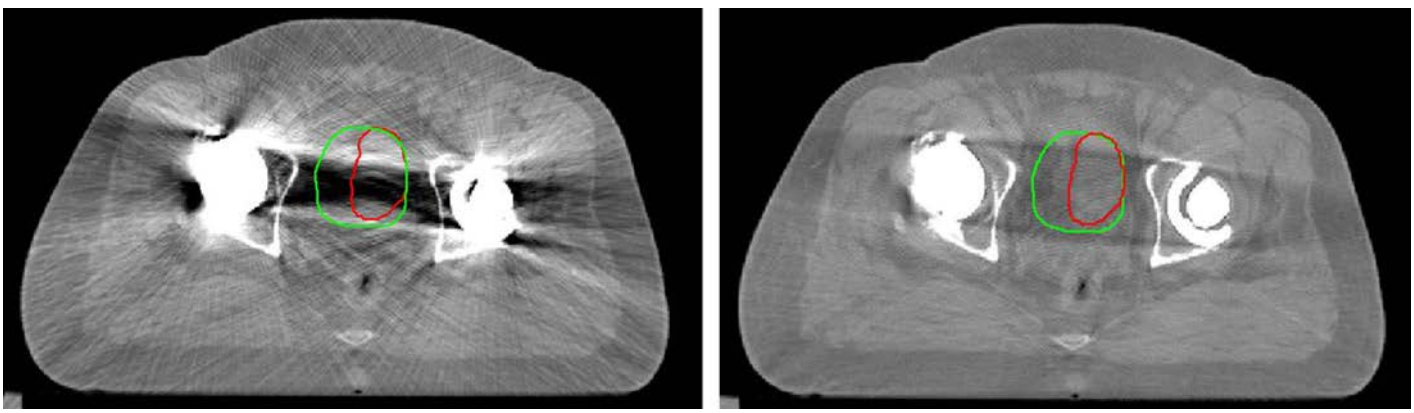

Uncorrected **O-MAR**

Volume difference 32%

Figure 13 Bladder contour. O-MAR contour in red. Uncorrected contour in green.

Contraindications

The O-MAR feature is optimized to correct for orthopedic metal implants that are embedded into normal tissue. There are instances (both orthopedic and non-orthopedic metal) where this approach can induce some minor artifacts. Therefore, in these cases the use of O-MAR is contraindicated. Basically, problems will occur when the metal is near air or low density tissue e.g. lung.

Below in Fig. 14, is an example where the metal protrudes beyond the skin boundary. In this case the O-MAR algorithm could erroneously cause the extension of the skin boundary. O-MAR should not be employed whenever metal extends beyond the skin.

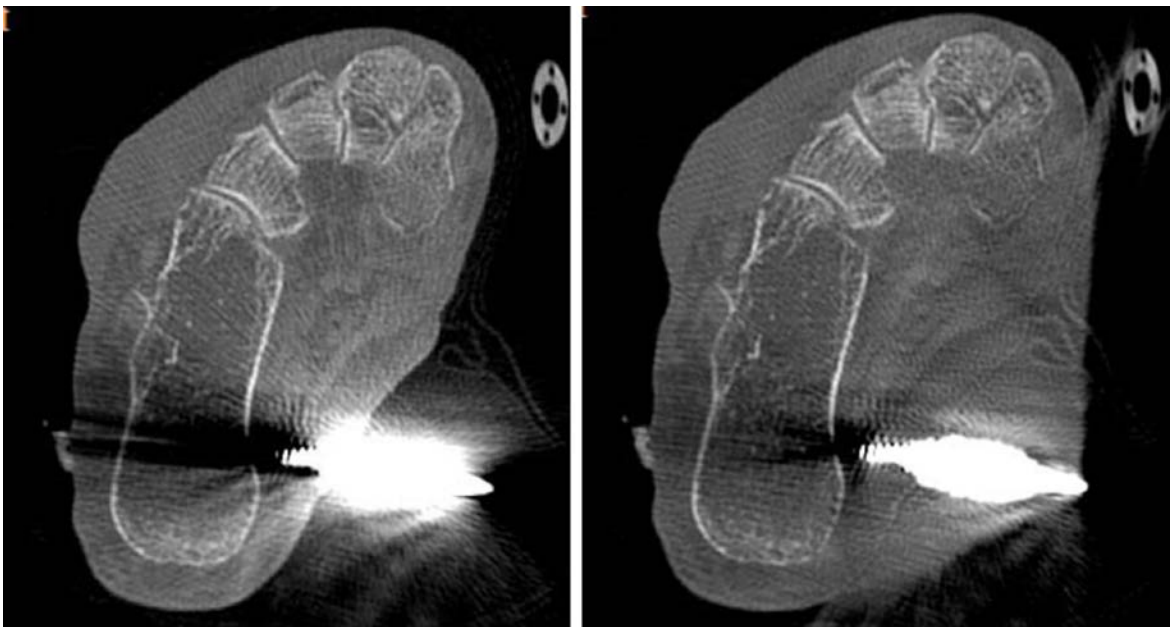

Figure 14 O-MAR image is on the right. Note, extension of foot tissue.

Metal screws in the spine can be problematic when using O-MAR. A slight degradation of the bone that is very near to the screws may occur with O-MAR. In Fig. 15, is an example of a spine L-2 slice that has two metal screws. Note, that part of the spinous process appears to be missing in the O-MAR image.

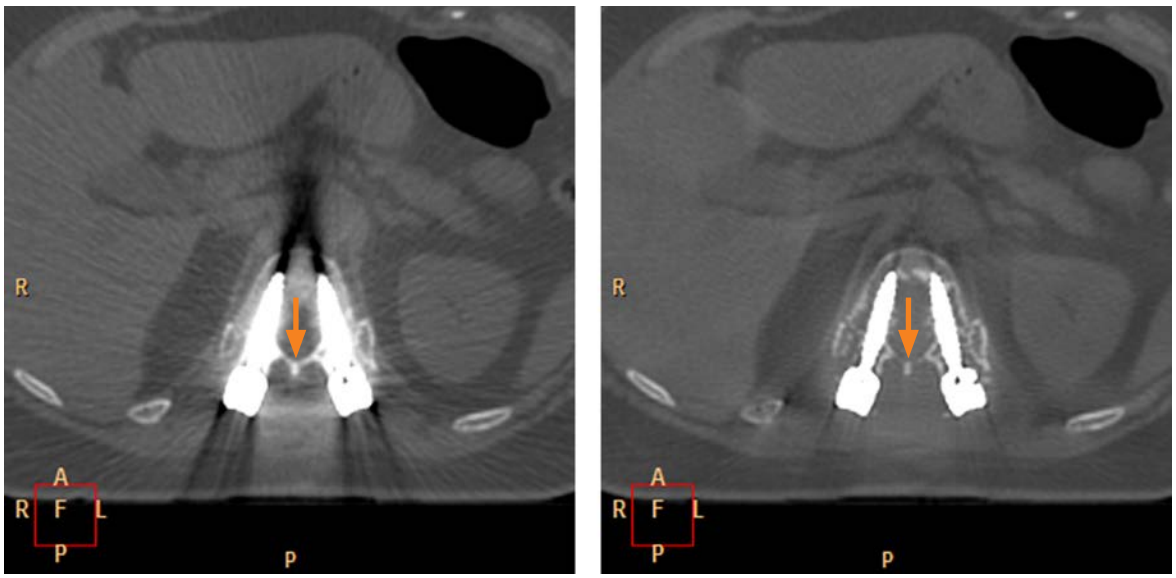

Figure 15 O-MAR Image is on the right. L-2 Spine.

Similar to air, lung tissue can sometimes confound the O-MAR process. In Fig. 16, there is an example where the algorithm induces some new streaks into the image.

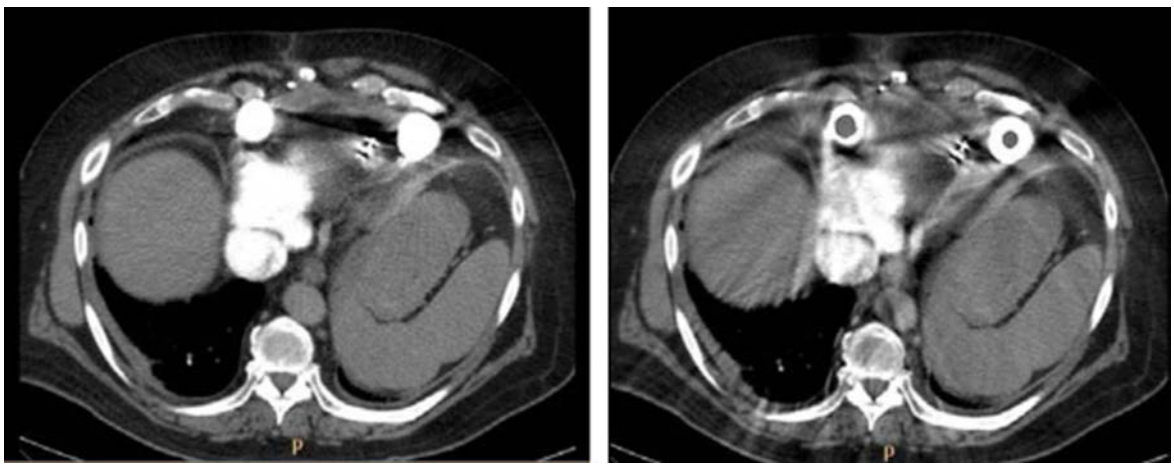

Figure 16 O-MAR on right. Note, new streaks inserted into image.

Pacemakers can be particularly problematic for O-MAR as shown in Fig. 17. Its proximity to the lung with metal wires entering the heart/lung area can cause O-MAR to induce streaking artifacts that are not present in the non-corrected image. Therefore, O-MAR is contraindicated for imaging any anatomy with pacemakers or pacemaker wires.

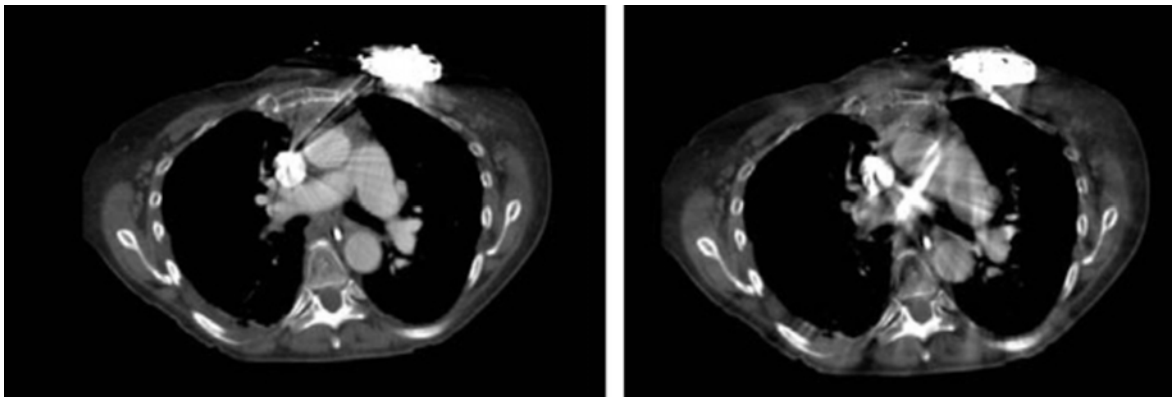

Figure 17 O-MAR is on the right.

Conclusions

In this paper, we have demonstrated numerous examples where the O-MAR algorithm is effective in reducing metal artifacts that are caused by orthopedic implants. With O-MAR, not only are severe streaking artifacts reduced, substantial portions of obscured anatomy can now be visualized. This will enable the clinician to formulate a more comprehensive and confident diagnosis. O-MAR also significantly facilitates contouring of tumors and critical structures, thus improving the workflow for Radiation Oncology applications.

There are some cases where O-MAR should be avoided as outlined in the contraindications section. These commonly occur when the metal is in close proximity to air or lung tissue or small metal object (e.g. stents) within iodinated contrast. Since there is an unforeseen consequence where O-MAR may induce some anomaly in the image, it behooves the clinician to always cross reference the uncorrected images with the O-MAR dataset. Since the system will always reconstruct both sets of images whenever O-MAR is selected, the uncorrected images are readily available. When O-MAR is utilized appropriately, it can improve the visualization of CT images that are negatively impacted by the presence of orthopedic metal.

References

1 G. Glover and N. Pelc "An algorithm for the reduction of metal clip artifacts in CT reconstructions." *Medical Physics 4*, 799-807 (1981)

2 R Brooks and G. Chiro "Correction for beam hardening in computed tomography." *Phys. Med. Biol.* 21, 390 (1976)

3 C. Ling, M. Schell et al. "CT-Assisted assessment of bladder and rectum dose in gynecological implants." *Int. J. Radiat. Oncol. Biol.* Phys.. 13, 1577-1582 (1987)

4 G. Wang D. Snyder and JA. O'Sullivan et al. "Iterative deblurring for CT metal artifact reduction." *IEEE Transact Med Imaging* 15, 657– 664. (1996)

5 XZ Lin, F. Miao et al. "High-definition CT Gemstone spectral imaging of the brain: initial results of selecting optimal monochromatic image for beam-hardening artifacts and image noise reduction." *J. Comput. Assist. Tomogr.* 35(2), 294-297 (2011)

Please visit www.philips.com/bigboreCT

© 2011 Koninklijke Philips Electronics N.V.
All rights are reserved.

Philips Healthcare reserves the right to make changes in specifications and/or to discontinue any product at any time without notice or obligation and will not be liable for any consequences resulting from the use of this publication.

Philips Healthcare is part of Royal Philips Electronics

www.philips.com/healthcare
healthcare@philips.com

Printed in The Netherlands
4522 962 82391 * DEC 2011